Cloud scavenging of anthropogenic refractory particles at a mountain site in North China

Lei Liu[1,2], Jian Zhang[1,2], Liang Xu[1,2], Qi Yuan[2], Dao Huang[2], Jianmin Chen[3], Zongbo Shi[4], Yele Sun[5], Pingqing Fu[5], Zifa Wang[5], Daizhou Zhang[6], Weijun Li[2,*]

[1]Environment Research Institute, Shandong University, Jinan 250100, China

[2]Department of Atmospheric Sciences, School of Earth Sciences, Zhejiang University, Hangzhou 320007, China

[3]Shanghai Key Laboratory of Atmospheric Particle Pollution and Prevention, Department of Environmental Science and Engineering, Fudan University, Shanghai 200433, China

[4]School of Geography, Earth and Environmental Sciences, University of Birmingham, Birmingham B15 2TT, UK

[5]State Key Laboratory of Atmospheric Boundary Layer Physics and Atmospheric Chemistry, Institute of Atmospheric Physics, Chinese Academy of Sciences, Beijing 100029, China

[6]Faculty of Environmental and Symbiotic Sciences, Prefectural University of Kumamoto, Kumamoto 862-8502, Japan

Correspondence to: Weijun Li (liweijun@zju.edu.cn)

Abstract. Aerosol-cloud interactions remain a major source of uncertainty in climate forcing estimate. Few studies have been conducted to characterize the aerosol-cloud interactions in heavily polluted conditions worldwide. In this study, cloud residual (cloud RES) and cloud interstitial (cloud INT) particles were collected during cloud events under different pollution levels from 22 July to 1 August, 2014 at Mt. Tai (1532 m above sea level) located in the North China Plain (NCP). Transmission electron microscopy (TEM) was used to investigate size and chemical composition of individual cloud RES and INT particles, and study the mixing states of these particles. Our results show that S-rich particles were predominant (78%) during clean periods (PM$_{2.5}$ < 15 μg m^{-3}), but a large amount of anthropogenic refractory particles (e.g., soot, fly ash, and metal) and their mixtures with S-rich particles (named as S-refractory) were observed during polluted periods. Cloud droplets collected during polluted periods were found to become an extremely complicated mixture by scavenging of abundant refractory particles. We found that 76% of cloud RES were S-refractory particles and that 26% of cloud RES contained two or more types of refractory particles. Soot-containing particles (i.e., S-soot and S-fly ash/metal-soot) were the most abundant (62%) among cloud RES, followed by fly ash/metal-containing particles (i.e., S-fly ash/metal and S-fly ash/metal-soot, 37%). The complicated cloud droplets have not been reported in clean continental or marine air before. Our findings provide an insight into the potential impacts on cloud radiative forcing from black carbon and metal catalyzed reactions of SO$_2$ in micro-cloud droplets containing soluble metals released from fly ash and metals over polluted air.

1. Introduction

Clouds play a crucial role in various physical and chemical processes occurring in the lower troposphere and hence affect the Earth's radiation budget (Seinfeld et al., 2016;Tilgner et al., 2014). Aerosol particles, including primary and secondary ones generated from natural and anthropogenic sources, either directly alter radiative forcing or act as cloud condensation nuclei (CCN) to indirectly influence it. At present, aerosol-cloud interactions unquestionably affect radiative forcing and global climate (McFiggans et al., 2006;Seinfeld and Pandis, 2006;Rosenfeld et al., 2014). CCN become cloud droplets through the condensation of water vapor when the relative humidity (RH) of an air parcel increases above saturation (Farmer et al., 2015). Size, chemical composition, and mixing state are main factors affecting the ability of a particle to act as CCN (Dusek et al., 2006;Li et al., 2011a;Fan et al., 2016;Rosenfeld, 2000;Hudson, 2007). In addition, aerosol particles incorporated into cloud droplets can be easily lifted into the free troposphere during cloud development and further extend their influence on cloud precipitation and regional climate (Fan et al., 2016).

Owing to the rapid industrialization and urbanization in Asia, large quantities of aerosol particles from anthropogenic sources are released into the atmosphere, which can dramatically affect the chemical composition of CCN, and furthermore change the properties of clouds such as radiative forcing, lifetime, and precipitation patterns (Li et al., 2011b;Drewnick et al., 2007;Ervens, 2015;Twohy and Anderson, 2008). High concentrations of aerosol particles increase the number of cloud droplets and reduce their size, which further results in the reduction of precipitation efficiency and in extending the lifetime of clouds (McFiggans et al., 2006;Qian et al., 2009;Fan et al., 2016;Li et al., 2017a;Rosenfeld, 2000). Moreover, anthropogenic aerosol particles - especially fly ash, metal, and soot particles - are incorporated into cloud droplets, and be transported long distances to affect ecosystems, human health, and radiative forcing (Li et al., 2013;Rosenfeld et al., 2014). Especially the toxic and bioaccumulative metals can deposit into the ecosystem following fog or precipitation and further cause severe health problems to human beings (Liu et al., 2012). Moreover, transition metals such as iron (Fe) and manganese (Mn) can enhance the in-cloud oxidation of sulfur dioxide to sulfate (Harris et al., 2013).

Recently, many studies have been performed worldwide to investigate aerosol-cloud interactions and the composition of cloud droplets. Schroder et al. (2015) investigated the activation of refractory

black carbon particles in stratocumulus clouds at a marine boundary layer site using a counterflow virtual impactor and single particle soot photometer. Ueda et al. (2014) reported the effects of in-cloud processes on the compositional changes of sea salt particles by collecting individual aerosol particles in and below clouds, respectively. Pierce et al. (2015) calculated size distribution changes and radiative forcing effects due to the scavenging of interstitial particles by cloud droplets in a clean, remote region. Roth et al. (2016) analyzed the composition and mixing state of cloud residues and out-of-cloud aerosol particles by single particle aerosol mass spectrometry on a mountain site and found that soot particles internally mixed with sulfate and nitrate were the dominant ones in cloud residues. All of the above studies were carried out in clean atmosphere; they could not observe the clear interactions between abundant anthropogenic particles and cloud droplets. However, the latest satellite observations indicated that large amounts of anthropogenic fine particles assembled in cloud base and might modify cloud properties in heavily polluted air influenced by industrial and urban emissions (Eck et al., 2018). Field observations are needed to confirm it and understand the interactions of aerosol-cloud over polluted areas, especially in North and South Asia.

Mt. Tai, the highest mountain in the NCP, is surrounded by several medium-sized industrial cities. The altitude of Mt. Tai is close to the top of the planetary boundary layer (PBL) above the NCP. Therefore, Mt. Tai is an ideal site to study the effects of regional transport and local emissions of anthropogenic aerosols on cloud properties. Numerous studies have been conducted on Mt. Tai, but virtually all the researchers mainly focus on the variation of chemical composition and size distribution of aerosol particles (Zhang et al., 2014) and chemical composition of cloud water (Li et al., 2017a;Wang et al., 2011). Because of the limitation of sampling and analyzing techniques, these studies did not consider the aerosol-cloud interactions at the top of Mt. Tai in North China.

Transmission electron microscopy (TEM) has become a powerful technique to characterize the morphology, composition, size, and mixing state of individual aerosol particles in recent years (Li et al., 2016a;Ueda et al., 2014). Many studies used single particle aerosol mass spectrometry (SPAMS) to characterize the composition and mixing state of residual particles of individual cloud droplets (Zhang et al., 2017;Lin et al., 2017;Pratt et al., 2010). Compared to the SPAMS, TEM can directly observe the morphology and mixing state of individual cloud droplet residual (cloud RES) and interstitial particles (cloud INT) (Ueda et al., 2014;Twohy and Anderson, 2008;Li et al., 2011a;Kojima et al., 2004). Therefore, TEM technique can not only be used to identify cloud RES and cloud INT collected in a

same cloud event but also reveal interactions between aerosol-clouds based on mixing state of individual particles. In this study, we collected individual particles during cloud events at the summit of Mt. Tai and applied TEM to obtain and compare the size, morphology, composition, and mixing state of cloud RES and cloud INT. This is helpful to understand the influence of anthropogenic sources on cloud properties above the heavily polluted region.

2. Experimental methods

2.1 Sampling sites

Field observations were carried out at Mt. Tai (36.251°N, 117.101°E; 1532 m above sea level (a.s.l)) from 22 July to 1 August 2014. Mt. Tai is the highest mountain in the central NCP and is surrounded by several medium-sized industrial cities (Fig. 1). A number of large coal-fired power plants, oil refinery plants, steel plants, and cement plants are located in these industrial cities (Jinan, Zibo, Laiwu, Liaocheng, Jining, Tai'an etc.) within a radius of 120 km around Mt. Tai (Fig. 1b). Jinan city is the capital of Shandong Province and is situated 60 km north of Mt. Tai. Tai'an city is located at the southern foot of Mt. Tai. Therefore, the local and regional emissions may have a large contribution to the air quality at the summit of Mt. Tai. Mt. Tai's altitude is close to the top of planetary boundary layer over the NCP, and local cloud events frequently occur at its summit, especially in summer.

As shown in Fig. 1c, individual particle samples were collected at a sampling site near the summit of Mt. Tai. The sampling site was usually covered by clouds when cloud events occurred during the sampling periods. The 24-h air mass backward trajectories arriving at Mt. Tai at 1500 m above ground level (a.g.l) (Fig. 1a) were calculated using the Hybrid Single-Particles Lagrangian Integrated Trajectory (HYSPLIT) model available at the NOAA Air Resources Laboratory's web server (Draxler and Rolph, 2003).
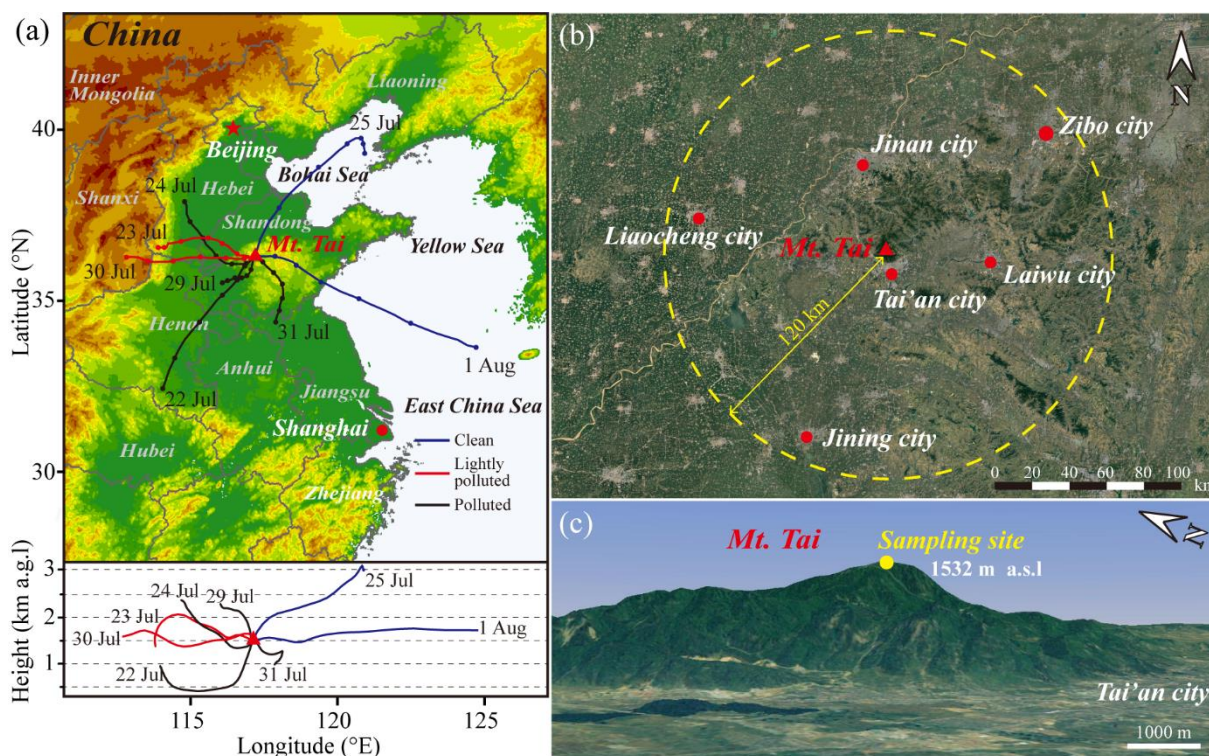
Figure 1. (a) Location of Mt. Tai in the North China Plain and the 24-h air mass backward trajectories arriving at Mt. Tai at 1500 m a.g.l during the sampling period. (b) The medium-sized industrial cities distributed within a radius of 120 km around Mt. Tai. (c) The expanded topographic view of Mt. Tai and the sampling site near the summit of Mt. Tai.

2.2 Individual particle collections

Individual aerosol particles were collected onto carbon films supported by TEM copper grids (carbon type-B, 300-mesh copper, Tianld Co., China) using a single-stage cascade impactor with a 0.5 mm diameter jet nozzle at a flow rate of 1.0 L min^{-1}. The aerodynamic diameter of particles collected with a 50% efficiency (cutoff diameter, d_{50}) by this individual sampler is 0.24 μm if particle density is 2 g cm^{-3}. More detailed information about the setup of a modified sampler can be found in Li et al. (2011a). When cloud events occurred at the summit of Mt. Tai, individual particle samples were collected during the cloud events except one cloud event in the late midnight of 26 July (Fig. 3). The sample information in the present study is listed in Table 1.

During the sampling period, meteorological data at the summit of Mt. Tai including pressure (P), relative humidity (RH), temperature (T), wind speed (WS), and wind direction (WD) were measured and recorded every 5 min by a pocket weather meter (Kestrel 4500, Nielsen-Kellermann Inc., USA). PM$_{2.5}$ concentrations on Mt. Tai were monitored on-line by a beta attenuation and optical analyzer

6

133   (model 5030 SHARP monitor, Thermo Scientific, USA).

134   **Table 1.** Information on individual particle samples collected on Mt. Tai.

| Sample ID	Sampling time (local time)	$PM_{2.5}$ ($\mu g\ m^{-3}$)	T (°C)	RH (%)	P (hPa)	WS ($m\ s^{-1}$)
1	22 Jul. 2014 16:04	51.6	22.8	100	849.1	0.9
2	23 Jul. 2014 08:00	24.2	20.4	100	849.4	2.5
3	24 Jul. 2014 07:43	74.3	19.2	100	848.0	0
4	25 Jul. 2014 17:00	11.8	13.9	100	838.0	5.5
5	29 Jul. 2014 16:18	72.9	20.8	95.7	848.0	1.1
6	30 Jul. 2014 19:24	24.2	17.5	100	844.2	0.8
7	31 Jul. 2014 17:30	56.4	18.1	100	849.0	0.9
8	01 Aug. 2014 17:56	14.7	18.8	100	849.1	1.8

135 **2.3 TEM analysis**

136   Individual aerosol particles collected on TEM grids were analyzed by a transmission electron

137 microscope (TEM, JEM-2100, JEOL Ltd., Japan) at a 200 kV accelerating voltage. TEM is equipped

138 with an energy-dispersive X-ray spectrometer (EDS, INCA X-Max[N] 80T, Oxford Instruments, UK).

139 EDS semi-quantitatively detects the elemental composition of individual particles with atomic number

140 greater than six ($Z > 6$). However, Cu peaks in the EDS spectra were not considered because of the

141 interference from the copper substrate of TEM grids. We acquired morphology, composition, and

142 mixing state of individual particles through the combination of TEM and EDS (TEM/EDS).

143   The distribution of aerosol particles on TEM grids was not uniform, with particle size decreasing

144 from the center to the edge of the TEM grids. Cloud droplets with larger size normally impacted on the

145 center and interstitial particles mostly distributed on the peripheral areas of TEM grids (Li et al., 2011a).

146 Moreover, cloud RES had large rims compared with cloud INT, suggesting that cloud RES were

147 droplets before being captured (Zhang et al., 2006). According to the distribution and morphology of

148 individual particles on the substrate, we can distinguish between cloud RES and cloud INT particles.

149 Figure 2 generally displays typical TEM images of cloud RES and cloud INT particles. Generally, a

150 number of previous studies using the cascade impactor have successfully captured individual interstitial

151 particles and cloud droplets on the substrate during cloud events (Ueda et al., 2014;Zhang et al.,

152 2006;Kojima et al., 2004;Li et al., 2011a).

153   To obtain the size of cloud RES and cloud INT particles, we measured the area and equivalent

154 circle diameter (ECD) of these analyzed particles by iTEM software (Olympus soft imaging solutions

155 GmbH, Germany). It should be noted that we measured ECD of the core of individual cloud RES

156 excluding the water rim because water rim only contains trace organics (Li et al., 2011a). The ECD can

157 be further converted to equivalent spherical diameter (ESD) according to the AFM analysis (refer to the

158 Supplement Fig. S1).
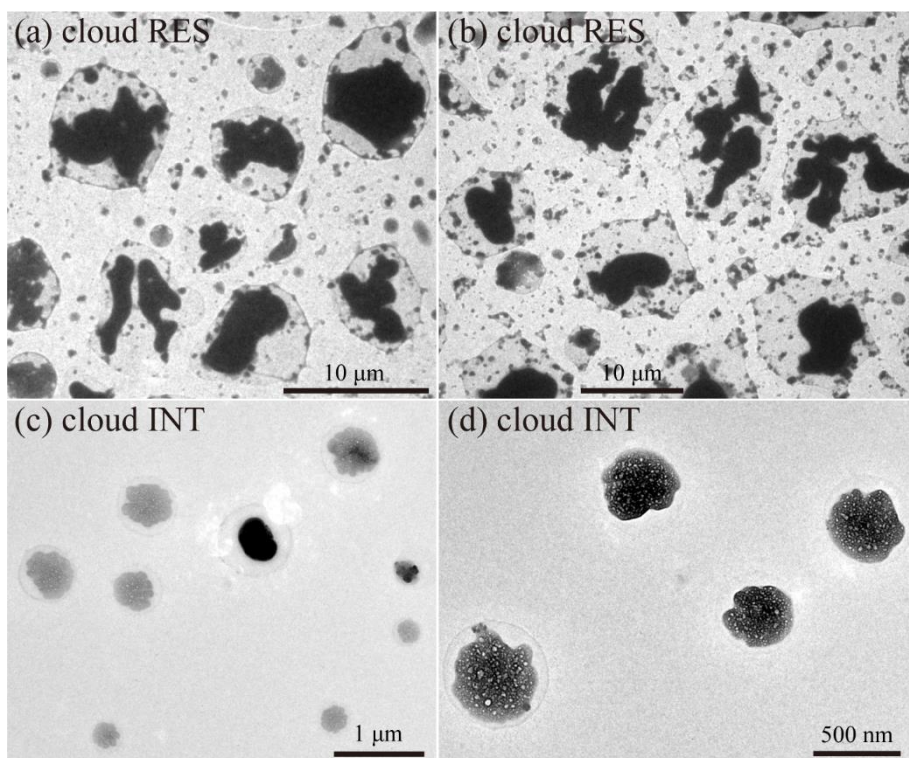
159

160 **Figure 2**. Low magnification TEM images of cloud RES (a-b) and cloud INT (c-d) particles collected

161 on Mt. Tai.

3. Results

3.1 Meteorological conditions and backward trajectories

Temporal variations of pressure (P), relative humidity (RH), temperature (T), wind speed (WS), wind direction (WD), and $PM_{2.5}$ concentration were measured on Mt. Tai from 22 July to 2 August 2014 (Fig. 3). During the sampling period, the temperature ranged from 12.6 to 29.4 $^{\circ}$C, and the RH varied between 48.2% and 100%. Each day during the sampling period, the RH reached 100% as temperatures decreased from the late afternoon into the evening (Fig. 3). We noticed that $PM_{2.5}$ concentrations on the mountaintop were closely related to wind direction and speed during the regional transport of hazes. Based on backward trajectories of air masses and $PM_{2.5}$ concentrations, the whole sampling period can be divided into three categories: *clean period* ($PM_{2.5} < 15$ μg m^{-3}), the prevailing winds were from the northeast to east and air masses were from higher altitudes above the marine areas which lead to the lowest $PM_{2.5}$ concentration; *lightly polluted period* (15 μg m^{-3} < $PM_{2.5}$ < 35 μg m^{-3}), the prevailing winds were from the west, and air masses originating from higher altitudes above continental areas brought regional pollutants to the summit of Mt. Tai; *polluted period* ($PM_{2.5} > 35$ μg m^{-3}), air masses originating from northwest, southwest, or south went through Tai'an city. Back trajectories as shown in Fig. 1a during polluted days suggest that air pollutants from industrialized cities might be lifted along the southern slope up to Mt. Tai's summit.
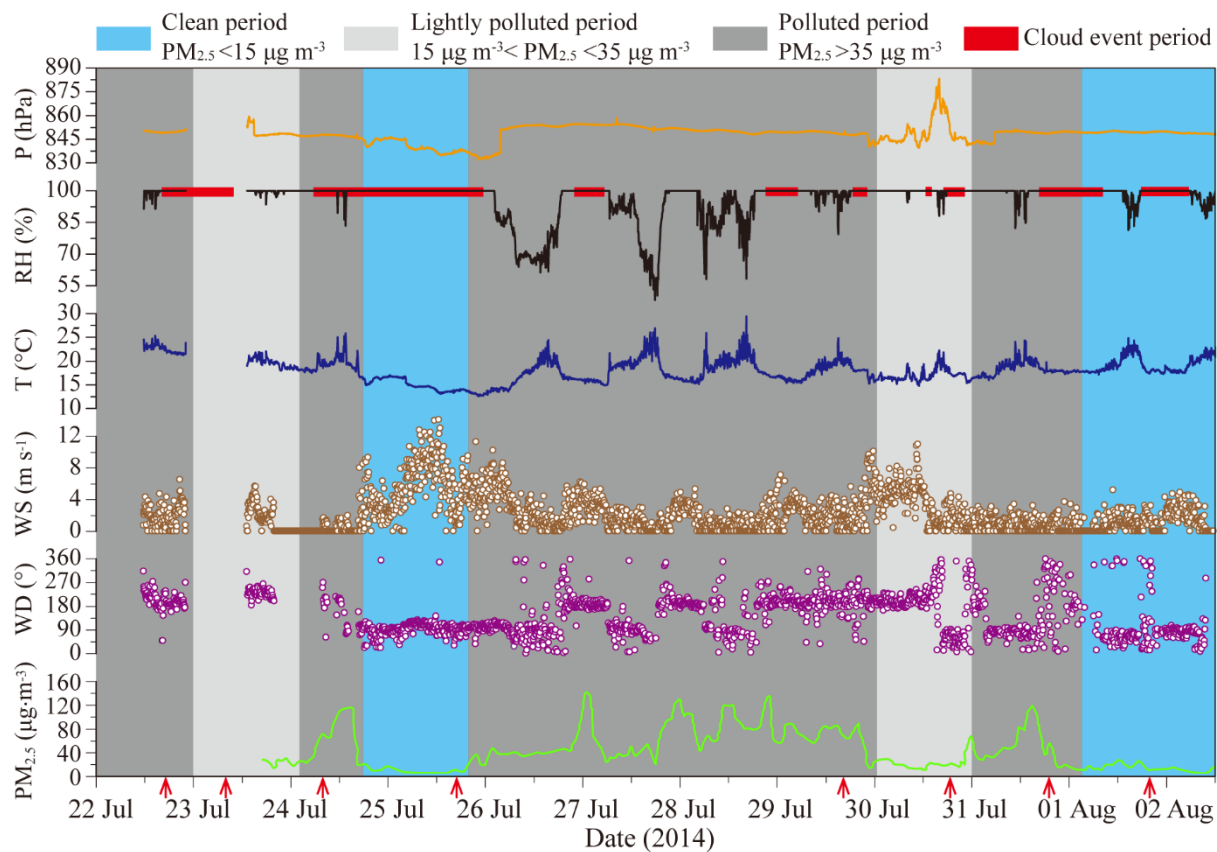
**Figure 3**. Temporal variations of pressure (P), relative humidity (RH), temperature (T), wind speed (WS), and wind direction (WD) measured on Mt. Tai from 22 July to 2 August 2014. The red arrows indicate collection times of individual particle samples during the cloud events.

3.2 Mixing state of anthropogenic refractory particles

Mixing state of aerosol particles is currently classified into population mixing state (Riemer and West, 2013) and single particle mixing state (Deng et al., 2014;Li et al., 2016b). Riemer and West (2013) defined the population mixing state as the distribution of the aerosol chemical species among the particles in a given population. However, based on the single particle mixing state of an individual particle acquired by TEM (Li et al., 2016b), this study emphasizes the distribution of different types of aerosol components within and on particle surface. Furthermore, single particle mixing state can be further divided into externally mixed particle and internally mixed particle (i.e., individual particles containing two or more types of aerosol components) (Li et al., 2016b).

Based on the elemental composition and morphology of individual particles, six basic types of externally mixed particles were classified: S-rich (Fig. S2a), soot (Fig. S2b), organic matter (OM, Fig. S2c), mineral (Fig. S2d), and fly ash/metal (Figs. S2e-h). The classification criteria of different particle types and their sources have been described in our previous study (Li et al., 2016a). S-rich particles representing secondary inorganic particles (e.g., SO_4^{2-}, NO_3^-, and NH_4^+) are transformed from gaseous SO_2, NO_x, and NH_3. OM can be divided into primary organic matter (POM) and secondary organic matter (SOM). POM is directly emitted from coal or biomass burning and normally has spherical or irregular shapes (Liu et al., 2017), whereas SOM is produced from the chemical oxidation of volatile organic compounds (VOCs) and exhibits OM-coating on S-rich particles (Li et al., 2016b). Fly ash (e.g., Si, Al, and O) and metal particles (e.g., Fe, Mn, Zn, and Pb) normally are emitted from coal-fired power plants and heavy industrial activities, such as production activities in steel mills and smelters. Soot particles are generated from incomplete combustion processes of biomass burning and fossil fuels in both industrial activities and vehicular emissions. In much of the climate-change and environmental literature, "soot" and "black carbon" are commonly used interchangeably, and "black carbon" is the most commonly used term in the climate-science community (Andreae and Gelencsér, 2006;Buseck et al., 2014). In the following sections, we use the term "soot" for the classification of particle types and the term "black carbon" for the discussion of the climate issues. Mineral particles come from construction activities, resuspended road dust, and natural soil. Among these types of particles, soot, POM, fly ash, mineral, and metal particles were refractory under electron beams and were thus termed as refractory particles (Ebert et al., 2016).

Based on the composition and mixing state of internally mixed particles (Figs. 4 and 5), they can be further classified into four categories: S-mineral (Figs. 4a and 5a), S-soot (Figs. 4b and 5b), S-fly ash/metal (Figs. 4c and 5c), S-fly ash/metal-soot (Figs. 4d and 5d). Here, these four types of particles with refractory inclusions are generally defined as "S-refractory" particles.
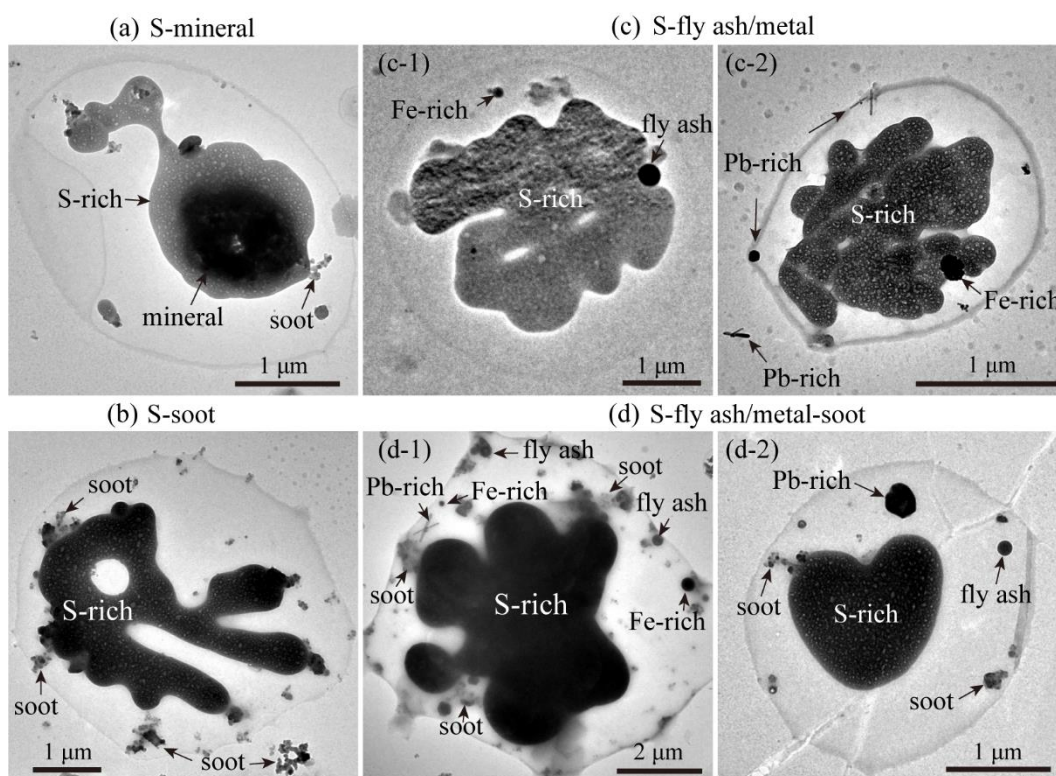
Figure 4. Typical TEM images of individual internally mixed cloud RES particles: (a) a mixture of S-rich and mineral; (b) a mixture of S-rich and soot; (c) a mixture of S-rich and fly ash/metal; (d) a mixture of S-rich, soot, and fly ash/metal.
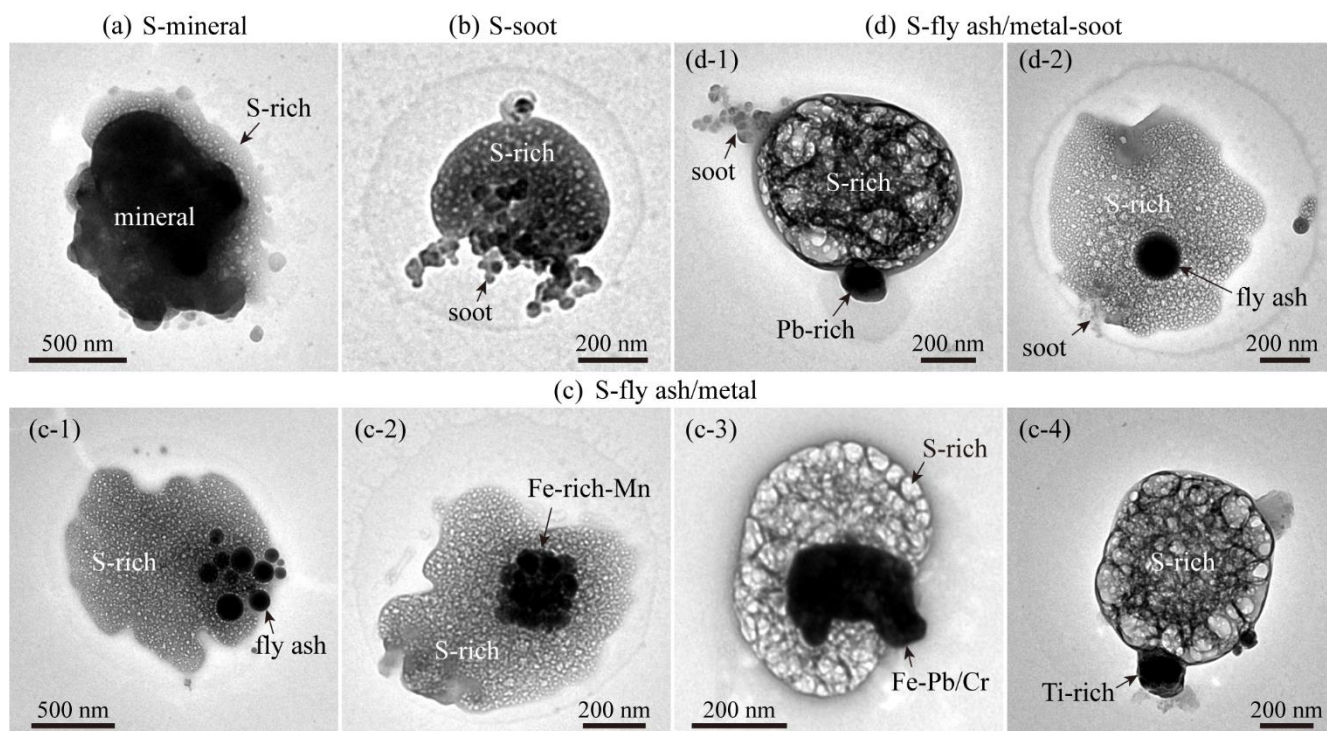
Figure 5. Typical TEM images of individual internally mixed cloud INT particles: (a) a mixture of S-rich and mineral; (b) a mixture of S-rich and soot; (c) a mixture of S-rich and fly ash/metal; (d) a mixture of S-rich, soot and fly ash/metal.
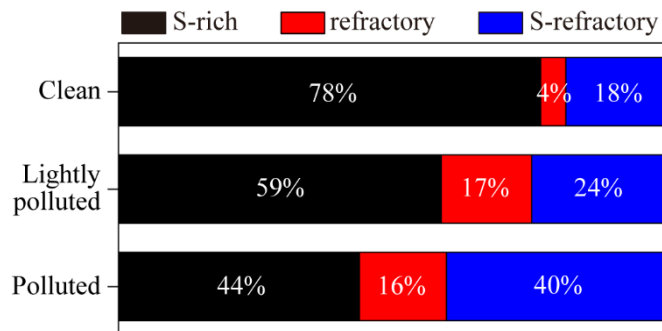
Figure 6 shows number fractions of S-rich, refractory, and S-refractory particles in clean, lightly polluted, and polluted periods on Mt. Tai. In clean periods, S-rich particles had the highest proportion (78%), followed by a 22% contribution of the refractory and S-refractory particles. This may be attributed to the clean air masses that originated from the clean marine area and arrived at the summit of Mt. Tai through high-altitude transport (above 1500 m) (Fig. 1). Because the air masses did not contact the ground surface, the local anthropogenic pollutants (e.g., soot, fly ash, and metal) could not be lifted to the summit of Mt. Tai. Hence, secondary particles like S-rich were dominant in the clean period. In the lightly polluted and polluted periods, the fraction of S-rich particles decreased to 59% and 44%, respectively; meanwhile, the fractions of refractory and S-refractory increased up to 41% and 56%, respectively (Fig. 6). The backward trajectories suggest that these air masses went through the most heavily polluted areas before they arrived at the mountaintop (Fig. 1). Air masses on two polluted days (e.g., 22 and 31 July) were lifted from ground level to the atmospheric boundary layer. Our study shows that number fractions of refractory and S-refractory particles significantly increased from clean to polluted periods (Fig. 6). This result shows that large amounts of primary refractory particles from

239 ground-level anthropogenic sources were lifted into the upper air and were further internally mixed with

240 S-rich particles.

241

242 **Figure 6.** Number fractions of S-rich, refractory, and S-refractory particles at different pollution levels.

3.3 Comparisons of cloud RES and INT particles

During the sampling period, a fog monitor was used to measure the size of cloud droplets during cloud events (Li et al., 2017a). This study reveals that in the cloud events all the cloud droplets displayed particle size larger than 2 μm in which size range the interstitial particles were absent. Based on their different size, we can know that these cloud droplets and interstitial particles impacted on different positions on the substrate. Although cloud droplets and interstitial particles became dry after the collection, they can still be identified based on the distribution and morphology of individual particles in TEM images (Li et al., 2011a;Ueda et al., 2014;Zhang et al., 2006;Kojima et al., 2004). Cloud RES display larger size and large rims around their CCN (Figs. 2 and 4) which has not been observed in non-cloud events. In contrast, cloud INT impacted on the position away from the center of sampling spot and their morphology looks like individual particles collected in non-cloud events. According to the rule, we can identify cloud RES and cloud INT in the samples collected during the cloud events.

Figure 7a shows that 100% of cloud RES and 83% of cloud INT contained S-rich species (i.e., S-rich and S-refractory). In other words, none of cloud RES were soot, fly ash/metal, and mineral particles but 17% of cloud INT were. Soot particles mainly distributed in the finer size bins (< 600 nm) of cloud INT (Fig. S3a). Interestingly, we found that 76% of cloud RES were a mixture of sulfates and refractory particles, which is 3.5 times of 22% in cloud INT (Fig. 7a). Furthermore, 26% of cloud RES had two or more types of inclusions (i.e., S-fly ash/metal-soot in Figs. 4d and 5d) but only 3% of cloud INT did. Therefore, we can conclude that cloud RES are extremely complex mixtures formed when cloud droplets act like a collector to scavenge these refractory particles.

The size-resolved number fractions of different particle types in cloud RES and cloud INT indicate that S-rich particles were predominant from 60 nm to 1.2 μm in cloud INT (Fig. S3a), and S-refractory particles (indicated by the red box) dominated from 400 nm to 5.5 μm in cloud RES (Fig. S3b). Figure 7b shows that the median diameters of cloud RES and cloud INT were 1.19 μm and 422 nm, respectively. The size of cloud RES was much larger than that of cloud INT, suggesting that size is an important factor affecting the CCN ability (Dusek et al., 2006).
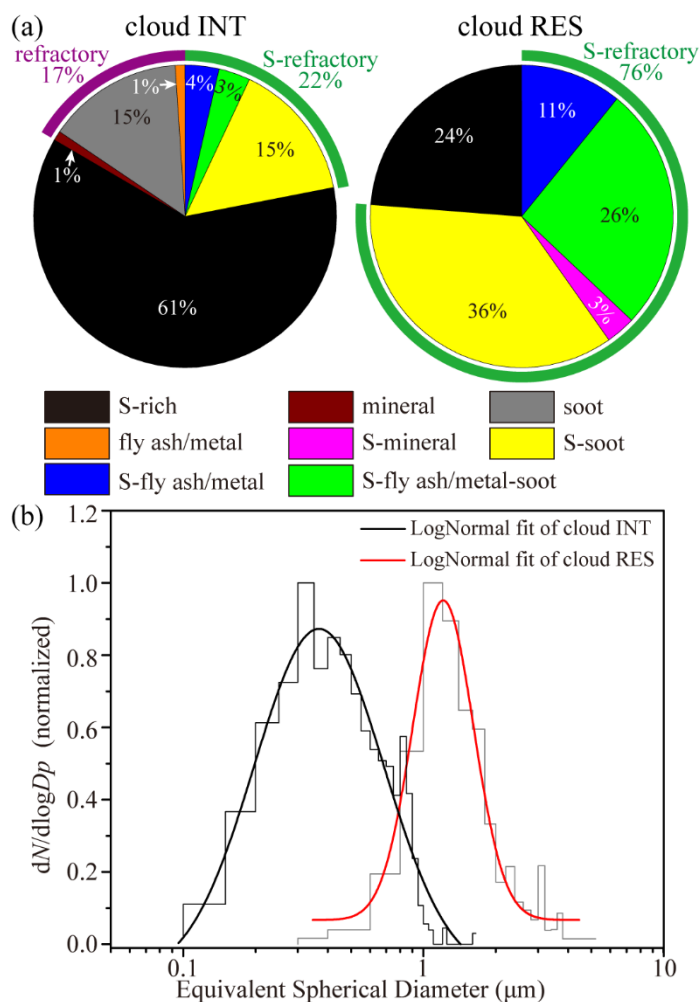
Figure 7. Number fractions of different particle types in cloud RES and INT particles (a) and size distributions of cloud RES and cloud INT particles (b). The measured particle sizes exclude the effects of water rims in TEM images. In total, 292 cloud RES and 1161 cloud INT particles were analyzed.

4. Discussion

TEM observations in this study reveal that cloud RES contained large amounts of refractory-containing particles primarily emitted from various anthropogenic sources in the heavily polluted NCP. As much as 76% of cloud RES were identified as S-refractory particles (Fig. 7a). We found that soot-containing particles (i.e., S-soot and S-fly ash/metal-soot) were the most abundant (62%) among the cloud RES, followed by the relatively abundant fly ash/metal-containing particles (i.e., S-fly ash/metal and S-fly ash/metal-soot, 37%) compared with 18% and 7% in the cloud INT, respectively (Fig. 7a). Although these refractory particles such as soot with hydrophobic properties could not be CCN directly, they can be easily accumulated by the existing cloud droplets as inclusions (Zuberi et al., 2005). In the heavily polluted NCP, large amounts of soot and fly ash/metal particles are released from anthropogenic sources (e.g., industrial activities and vehicular exhaust). During cloud events, abundant

refractory particles can be efficiently entrained into existing liquid cloud droplets by wet scavenging. Li et al. (2011a) reported that particle number decreased dramatically during cloud formation at Mt. Tai with a scavenging ratio of 0.54, which demonstrated that aerosol particles could efficiently be incorporated into cloud droplets. Physical coagulation of interstitial particles with cloud droplets is an important process in developing clouds, which can lead to the reduction of cloud INT number and a size increase of cloud RES after the cloud dries (Pierce et al., 2015). As we know so far, the extremely complicated mixture of secondary and primary particles observed in the present study has seldom been found in cloud droplets in clean air over developed countries (Ueda et al., 2014;Schneider et al., 2017;Hao et al., 2013;Kojima et al., 2004), remote areas (Hiranuma et al., 2013), and ocean (Twohy and Anderson, 2008;Hopkins et al., 2008;Zhang et al., 2006). For example, Zhang et al. (2006) reported that S-rich particles were predominant in the cloud RES with a small number fraction of sea salt particles over the Sea of Japan and soot or fly ash/metal particles were not observed. The present study reveals that individual cloud droplets are a far more complicated system in polluted air in North China than in the pristine continental and clean ocean air of the world.

The cloud properties such as albedo and lifetimes could be largely modified by the aerosol-cloud interactions, especially in heavily polluted regions (Wang et al., 2010;Wang et al., 2013). The model simulation revealed that black carbon aerosols had a noticeable impact (up to nearly 20%) on cloud droplet number concentration in polluted black carbon source regions (Cherian et al., 2017). Especially, abundant black carbon particles incorporated into cloud droplets could lead to a decrease in cloud albedo by absorbing radiation and an increase of temperature in troposphere, then accelerate the evaporation of the cloud droplets (Zuberi et al., 2005;Ackerman et al., 2000;Adachi et al., 2010;Wang et al., 2013). In the past few decades, precipitation was significantly reduced over east-central China due to the large amounts of anthropogenic aerosols (Zhao et al., 2006;Qian et al., 2009). Because an excess of aerosols in clouds could reduce precipitation, the non-precipitating clouds in the NCP tend to evaporate back to aerosol particles by solar radiation. It is highly probable that abundant black carbon particles presenting in the cloud droplets in the heavily polluted NCP in this study (e.g., particle 1 and 2 in Fig. 8) significantly affected the cloud properties and regional climate.

Fly ash and metal particles are a typical "fingerprint" pointing to the coal-fired power plants and boilers in factories and heavy industries (e.g., steel plant and smelting factory) (Chen et al., 2012;Moffet et al., 2008;Li et al., 2016a). Indeed, the most intense emissions from various industries in the world

occur in Hebei and Shandong provinces in the NCP (Qi et al., 2017). It is well known that these industrial activities continuously release anthropogenic pollutants via high stacks into the upper air. Liu et al. (2012) reported that the concentration of Zn reached 249.1 μg L^{-1} in the cloud/fog water samples at Mt. Tai, followed by Al (157.3 μg L^{-1}), Fe (105.8 μg L^{-1}), Pb (46.2 μg L^{-1}), and Mn (42.8 μg L^{-1}), which were extremely higher than those values reported at Mt. Schmücke in Germany (Fomba et al., 2015). Combining these results with our present study, we infer that fine primary particles emitted from these industrial activities might spread and be lifted to the upper air more easily than at ground level. These metal particles, especially Pb and Zn of nanometer size, can harm ecosystems and human health (Roberts et al., 2004). The fly ash and metal particles incorporated into cloud droplets (e.g., particle 1 in Fig. 8) could go through the atmospheric acid Fe dissolution processes during long-range transport reported by Li et al. (2017b). If they were further transported to remote oceanic regions, soluble Fe species in the aerosol particles can fertilize plankton on the surface of ocean (Li et al., 2017b;Ito and Shi, 2016). Therefore, these anthropogenic fly ash/metal particles in polluted air contaminate cloud droplets and further amplify potential impacts of fine metal particles on the biogeochemical cycle in the troposphere.

Some studies suggested that the aqueous oxidation of SO$_2$ to sulfate by H$_2$O$_2$ and O$_3$ in cloud droplets was dominant at Mt. Tai (Shen et al., 2012). However, cloud water collected on Mt. Tai contained high concentrations of soluble Fe, Mn, Zn, and Pb (Liu et al., 2012). These soluble metals in cloud droplets are released from aqueous reactions between metal particles and acidic sulfates in cloud droplets (Li et al., 2017b). Harris et al. (2013) estimated that the oxidation of SO$_2$ in cloud droplets catalyzed by natural transition metal ions (TMIs) in mineral dust was dominant at Mt. Schmücke in Germany. For this study, how the soluble anthropogenic TMIs drive sulfate formation through TMI catalysis in micro-cloud droplets is still unresolved in polluted air. We propose that anthropogenic TMI catalysis contributing to sulfate production should be further studied in cloud droplets in the polluted NCP.
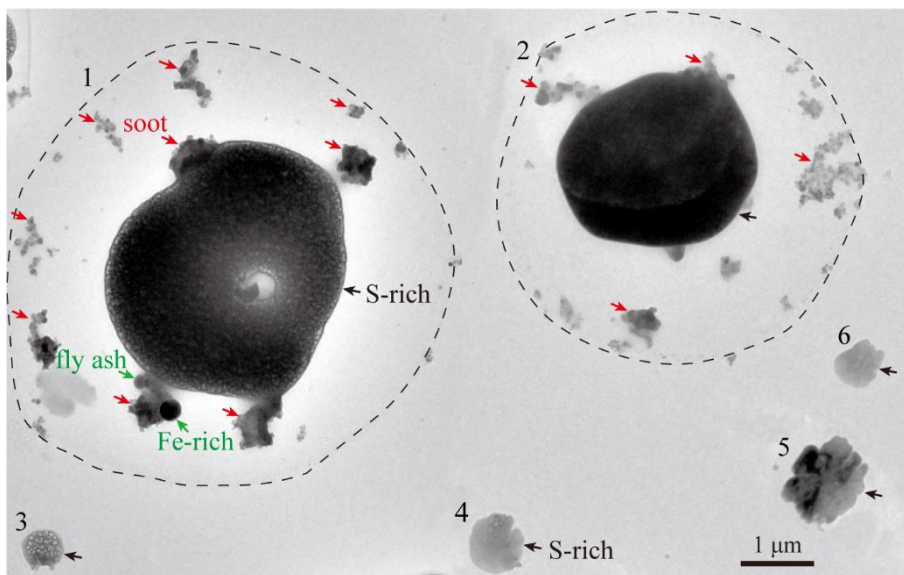
Figure 8. TEM image of cloud RES and INT particles collected during the cloud event occurred on the polluted day of 31 July. Particle 1 and 2 are cloud RES and particle 3, 4, 5, and 6 are cloud INT. The dashed lines indicate the water rims that were left after the cloud droplets impacting on the substrate become dry.

The non-precipitating cloud processes over the polluted air of NCP quickly change the mixing state and composition of aerosol and cloud droplets in the upper air, potentially causing various effects such as human health, regional climate, and biogeochemical cycle at the larger regional scale. To better understand the aerosol-cloud interactions in this study, we offer the conceptual model of Fig. 9. The tall stacks of plants can emit smoke plumes that contain fine refractory particles and gaseous pollutants to the upper air. A portion of particles in urban areas can also be lifted to the mountaintop by prevailing valley winds. Once the clouds form on a mountaintop (or later are transported in other directions), these cloud droplets act as collectors to scavenge the refractory particles. These refractory particles as inclusions might complicate the cloud chemistry in micro-cloud droplets. Gaseous pollutants such as SO_2, NO_x, and VOCs may have enhanced aqueous oxidation potential in the complex cloud droplets. Our study is designed to better understand the aerosol-cloud interactions on the mountaintop in polluted industrial and urban areas. Recently, a study showed that the major aerosol pollution events with very high fine mode AOD (>1.0 in mid-visible) in the China-Korea-Japan region are often observed to be associated with significant cloud cover (Eck et al., 2018). Therefore, we expect that large amounts of fine refractory particles from polluted areas scavenging in clouds have important impacts not only at

361　local but also in large regional scale.
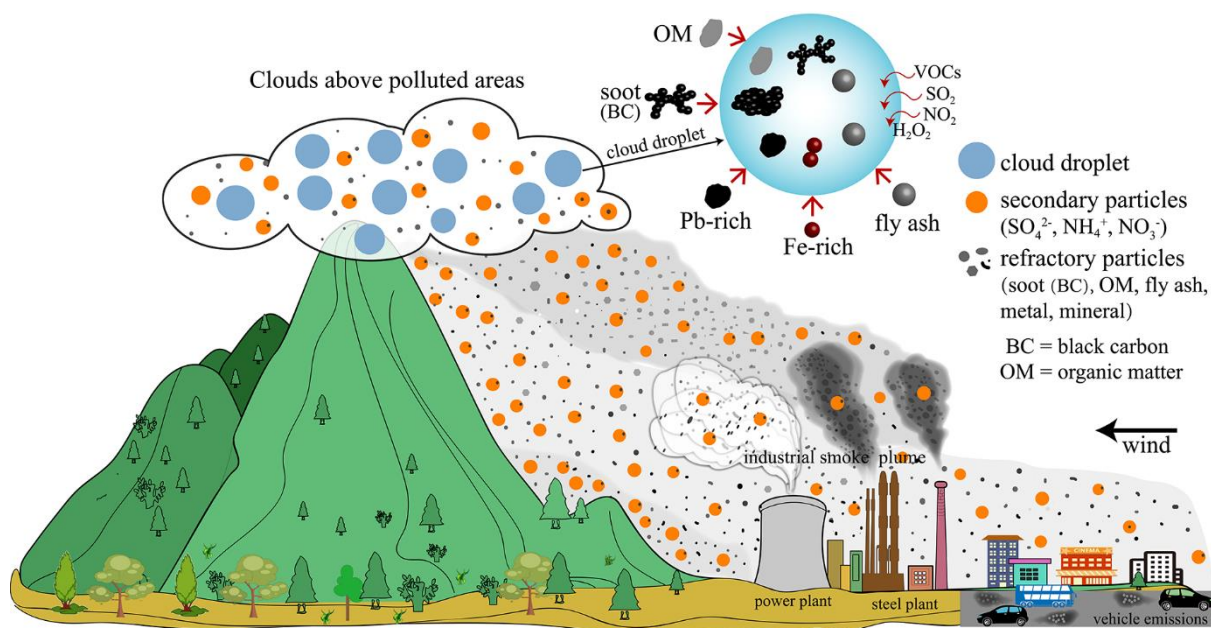
Figure 9. A conceptual model illustrating mechanisms of aerosol-cloud interactions on mountaintop influenced by anthropogenic pollutants from heavy industrial and urban emissions.

5. Conclusions

Individual aerosol particles were collected during cloud events on Mt. Tai from 22 July to 1 August, 2014. Cloud RES and INT particles were separated by their distribution on TEM grids and their composition was identified by TEM/EDS. Individual particles were classified into S-rich, refractory (i.e., mineral, soot, fly ash/metal) and S-refractory (i.e., S-mineral, S-soot, S-fly ash/metal, and S-fly ash/metal-soot). According to air mass backward trajectories and $PM_{2.5}$ concentrations on Mt. Tai, the entire sampling period was divided into three classes: a clean period ($PM_{2.5} < 15$ μg m^{-3}), a lightly polluted period (15 μg m^{-3} $< PM_{2.5} < 35$ μg m^{-3}), and a polluted period ($PM_{2.5} > 35$ μg m^{-3}). In the clean period, individual particles were dominated by S-rich particles (78%), whereas the fraction of refractory particles and S-refractory particles increased significantly and dominated during the polluted periods. This suggested that anthropogenic pollutants from tall stacks of coal-fired power plants and heavy industries and vehicular exhaust in cities could be lifted to the summit of Mt. Tai under the prevailing southerly winds in summer.

TEM observations showed that 76% of cloud RES were S-refractory particles contaminated by anthropogenic refractory particles, compared with only 22% of cloud INT. Cloud RES displayed a larger size than cloud INT, which indicates that particle size decidedly affects CCN ability. Our study

20

381 reveals that large amounts of anthropogenic refractory particles were incorporated into cloud droplets

382 through in-cloud processes. Especially important is that abundant black carbon particles in cloud

383 droplets could alter radiative forcing of clouds and accelerate the evaporation of cloud droplets. The

384 high concentrations of transition metal ions might favor the aqueous-phase oxidation of SO_2 by O_2 in

385 cloud droplets under the heavily polluted conditions in the NCP. Fly ash/metal-containing cloud

386 droplets could be transported long distance and harm ecosystems and human health through wet

387 deposition. We propose a conceptual model to show the aerosol-cloud interactions on mountaintops

388 influenced by heavily polluted air.

389

390 **Data availability.** All data presented in this paper are available upon request. Please contact the

391 corresponding author (liweijun_atmos@gmail.com).

392

393 **Competing interests.** The authors declare that they have no conflict of interest.

394

References

Ackerman, A. S., Toon, O. B., Stevens, D. E., Heymsfield, A. J., Ramanathan, V., and Welton, E. J.: Reduction of tropical cloudiness by soot, Science, 288, 1042-1047, 10.1126/science.288.5468.1042, 2000.

Adachi, K., Chung, S. H., and Buseck, P. R.: Shapes of soot aerosol particles and implications for their effects on climate, J. Geophys. Res.-Atmos., 115, D15206, 10.1029/2009JD012868, 2010.

Andreae, M. O., and Gelencsér, A.: Black carbon or brown carbon? The nature of light-absorbing carbonaceous aerosols, Atmos. Chem. Phys., 6, 3131-3148, 10.5194/acp-6-3131-2006, 2006.

Buseck, P. R., Adachi, K., Gelencsér, A., Tompa, É., and Pósfai, M.: Ns-Soot: A Material-Based Term for Strongly Light-Absorbing Carbonaceous Particles, Aerosol Sci. Tech., 48, 777-788, 10.1080/02786826.2014.919374, 2014.

Chen, H., Laskin, A., Baltrusaitis, J., Gorski, C. A., Scherer, M. M., and Grassian, V. H.: Coal Fly Ash as a Source of Iron in Atmospheric Dust, Environ. Sci. Technol., 46, 2112-2120, 10.1021/es204102f, 2012.

Cherian, R., Quaas, J., Salzmann, M., and Tomassini, L.: Black carbon indirect radiative effects in a climate model, Tellus Ser. B-Chem. Phys. Meteorol., 69, 10.1080/16000889.2017.1369342, 2017.

Deng, C., Brooks, S. D., Vidaurre, G., and Thornton, D. C. O.: Using Raman Microspectroscopy to Determine Chemical Composition and Mixing State of Airborne Marine Aerosols over the Pacific Ocean, Aerosol Sci. Tech., 48, 193-206, 10.1080/02786826.2013.867297, 2014.

Draxler, R. R., and Rolph, G. D.: HYSPLIT (HYbrid Single-Particle Lagrangian Integrated Trajectory) Model access via NOAA ARL READY Website, http://ready.arl.noaa.gov/HYSPLIT.php, NOAA Air Resources Laboratory, Silver Spring, MD, 2003.

Drewnick, F., Schneider, J., Hings, S. S., Hock, N., Noone, K., Targino, A., Weimer, S., and Borrmann, S.: Measurement of ambient, interstitial, and residual aerosol particles on a mountaintop site in central Sweden using an aerosol mass spectrometer and a CVI, J. Atmos. Chem., 56, 1-20, 10.1007/s10874-006-9036-8, 2007.

Dusek, U., Frank, G., Hildebrandt, L., Curtius, J., Schneider, J., Walter, S., Chand, D., Drewnick, F., Hings, S., and Jung, D.: Size matters more than chemistry for cloud-nucleating ability of aerosol particles, Science, 312, 1375-1378, 10.1126/science.1125261, 2006.

429 Ebert, M., Weigel, R., Kandler, K., Günther, G., Molleker, S., Grooß, J. U., Vogel, B., Weinbruch, S.,

430 and Borrmann, S.: Chemical analysis of refractory stratospheric aerosol particles collected within the

431 arctic vortex and inside polar stratospheric clouds, Atmos. Chem. Phys., 16, 8405-8421,

432 10.5194/acp-16-8405-2016, 2016.

433 Eck, T. F., Holben, B. N., Reid, J. S., Xian, P., Giles, D. M., Sinyuk, A., Smirnov, A., Schafer, J. S.,

434 Slutsker, I., Kim, J., Koo, J. H., Choi, M., Kim, K. C., Sano, I., Arola, A., Sayer, A. M., Levy, R. C.,

435 Munchak, L. A., O'Neill, N. T., Lyapustin, A., Hsu, N. C., Randles, C. A., Da Silva, A. M., Buchard, V.,

436 Govindaraju, R. C., Hyer, E., Crawford, J. H., Wang, P., and Xia, X.: Observations of the Interaction

437 and Transport of Fine Mode Aerosols With Cloud and/or Fog in Northeast Asia from Aerosol Robotic

438 Network (AERONET) and Satellite Remote Sensing, J. Geophys. Res.-Atmos., 123, 5560-5587,

439 10.1029/2018JD028313, 2018.

440 Ervens, B.: Modeling the Processing of Aerosol and Trace Gases in Clouds and Fogs, Chem. Rev., 115,

441 4157-4198, 10.1021/cr5005887, 2015.

442 Fan, J., Wang, Y., Rosenfeld, D., and Liu, X.: Review of Aerosol-Cloud Interactions: Mechanisms,

443 Significance, and Challenges, J. Atmos. Sci., 73, 4221-4252, 10.1175/jas-d-16-0037.1, 2016.

444 Farmer, D. K., Cappa, C. D., and Kreidenweis, S. M.: Atmospheric Processes and Their Controlling

445 Influence on Cloud Condensation Nuclei Activity, Chem. Rev., 115, 4199-4217, 10.1021/cr5006292,

446 2015.

447 Fomba, K. W., van Pinxteren, D., Muller, K., Iinuma, Y., Lee, T., Collett, J. L., and Herrmann, H.: Trace

448 metal characterization of aerosol particles and cloud water during HCCT 2010, Atmos. Chem. Phys., 15,

449 8751-8765, 10.5194/acp-15-8751-2015, 2015.

450 Hao, L., Romakkaniemi, S., Kortelainen, A., Jaatinen, A., Portin, H., Miettinen, P., Komppula, M.,

451 Leskinen, A., Virtanen, A., Smith, J. N., Sueper, D., Worsnop, D. R., Lehtinen, K. E. J., and Laaksonen,

452 A.: Aerosol Chemical Composition in Cloud Events by High Resolution Time-of-Flight Aerosol Mass

453 Spectrometry, Environ. Sci. Technol., 47, 2645-2653, 10.1021/es302889w, 2013.

454 Harris, E., Sinha, B., van Pinxteren, D., Tilgner, A., Fomba, K. W., Schneider, J., Roth, A., Gnauk, T.,

455 Fahlbusch, B., and Mertes, S.: Enhanced role of transition metal ion catalysis during in-cloud oxidation

456 of SO_2, Science, 340, 727-730, 10.1126/science.1230911, 2013.

457 Hiranuma, N., Brooks, S. D., Moffet, R. C., Glen, A., Laskin, A., Gilles, M. K., Liu, P., Macdonald, A.

458 M., Strapp, J. W., and McFarquhar, G. M.: Chemical characterization of individual particles and

residuals of cloud droplets and ice crystals collected on board research aircraft in the ISDAC 2008 study, J. Geophys. Res.-Atmos., 118, 6564-6579, 10.1002/jgrd.50484, 2013.

Hopkins, R. J., Desyaterik, Y., Tivanski, A. V., Zaveri, R. A., Berkowitz, C. M., Tyliszczak, T., Gilles, M. K., and Laskin, A.: Chemical speciation of sulfur in marine cloud droplets and particles: Analysis of individual particles from the marine boundary layer over the California current, J. Geophys. Res.-Atmos., 113, D04209, 10.1029/2007jd008954, 2008.

Hudson, J. G.: Variability of the relationship between particle size and cloud-nucleating ability, Geophys. Res. Lett., 34, L08801, 10.1029/2006gl028850, 2007.

Ito, A., and Shi, Z.: Delivery of anthropogenic bioavailable iron from mineral dust and combustion aerosols to the ocean, Atmos. Chem. Phys., 16, 85-99, 10.5194/acp-16-85-2016, 2016.

Kojima, T., Buseck, P. R., Wilson, J. C., Reeves, J. M., and Mahoney, M. J.: Aerosol particles from tropical convective systems: Cloud tops and cirrus anvils, J. Geophys. Res.-Atmos., 109, D12201, 10.1029/2003JD004504, 2004.

Li, J., Wang, X., Chen, J., Zhu, C., Li, W., Li, C., Liu, L., Xu, C., Wen, L., Xue, L., Wang, W., Ding, A., and Herrmann, H.: Chemical composition and droplet size distribution of cloud at the summit of Mount Tai, China, Atmos. Chem. Phys., 17, 9885-9896, 10.5194/acp-17-9885-2017, 2017a.

Li, W., Li, P., Sun, G., Zhou, S., Yuan, Q., and Wang, W.: Cloud residues and interstitial aerosols from non-precipitating clouds over an industrial and urban area in northern China, Atmos. Environ., 45, 2488-2495, 10.1016/j.atmosenv.2011.02.044, 2011a.

Li, W., Zhang, D., Shao, L., Zhou, S., and Wang, W.: Individual particle analysis of aerosols collected under haze and non-haze conditions at a high-elevation mountain site in the North China plain, Atmos. Chem. Phys., 11, 11733-11744, 10.5194/acp-11-11733-2011, 2011b.

Li, W., Wang, Y., Collett, J. L., Chen, J., Zhang, X., Wang, Z., and Wang, W.: Microscopic Evaluation of Trace Metals in Cloud Droplets in an Acid Precipitation Region, Environ. Sci. Technol., 47, 4172-4180, 10.1021/es304779t, 2013.

Li, W., Shao, L., Zhang, D., Ro, C.-U., Hu, M., Bi, X., Geng, H., Matsuki, A., Niu, H., and Chen, J.: A review of single aerosol particle studies in the atmosphere of East Asia: morphology, mixing state, source, and heterogeneous reactions, J. Clean Prod., 112, 1330-1349, 10.1016/j.jclepro.2015.04.050, 2016a.

Li, W., Sun, J., Xu, L., Shi, Z., Riemer, N., Sun, Y., Fu, P., Zhang, J., Lin, Y., and Wang, X.: A

conceptual framework for mixing structures in individual aerosol particles, J. Geophys. Res.-Atmos.,
121, 13784-13798, 10.1002/2016JD025252, 2016b.

Li, W., Xu, L., Liu, X., Zhang, J., Lin, Y., Yao, X., Gao, H., Zhang, D., Chen, J., and Wang, W.: Air
pollution–aerosol interactions produce more bioavailable iron for ocean ecosystems, Sci. Adv., 3,
e1601749, 10.1126/sciadv.1601749, 2017b.

Lin, Q., Zhang, G., Peng, L., Bi, X., Wang, X., Brechtel, F. J., Li, M., Chen, D., Peng, P., Sheng, G., and
Zhou, Z.: In situ chemical composition measurement of individual cloud residue particles at a mountain
site, southern China, Atmos. Chem. Phys., 17, 8473-8488, 10.5194/acp-17-8473-2017, 2017.

Liu, L., Kong, S., Zhang, Y., Wang, Y., Xu, L., Yan, Q., Lingaswamy, A. P., Shi, Z., Lv, S., Niu, H., Shao,
L., Hu, M., Zhang, D., Chen, J., Zhang, X., and Li, W.: Morphology, composition, and mixing state of
primary particles from combustion sources — crop residue, wood, and solid waste, Sci. Rep., 7, 5047,
10.1038/s41598-017-05357-2, 2017.

Liu, X., Wai, K. M., Wang, Y., Zhou, J., Li, P., Guo, J., Xu, P., and Wang, W.: Evaluation of trace
elements contamination in cloud/fog water at an elevated mountain site in Northern China,
Chemosphere, 88, 531-541, 10.1016/j.chemosphere.2012.02.015, 2012.

McFiggans, G., Artaxo, P., Baltensperger, U., Coe, H., Facchini, M. C., Feingold, G., Fuzzi, S., Gysel,
M., Laaksonen, A., Lohmann, U., Mentel, T. F., Murphy, D. M., O'Dowd, C. D., Snider, J. R., and
Weingartner, E.: The effect of physical and chemical aerosol properties on warm cloud droplet
activation, Atmos. Chem. Phys., 6, 2593-2649, 10.5194/acp-6-2593-2006, 2006.

Moffet, R. C., Desyaterik, Y., Hopkins, R. J., Tivanski, A. V., Gilles, M. K., Wang, Y., Shutthanandan, V.,
Molina, L. T., Abraham, R. G., Johnson, K. S., Mugica, V., Molina, M. J., Laskin, A., and Prather, K. A.:
Characterization of Aerosols Containing Zn, Pb, and Cl from an Industrial Region of Mexico City,
Environ. Sci. Technol., 42, 7091-7097, 10.1021/es7030483, 2008.

Pierce, J., Croft, B., Kodros, J., D'Andrea, S., and Martin, R.: The importance of interstitial particle
scavenging by cloud droplets in shaping the remote aerosol size distribution and global aerosol-climate
effects, Atmos. Chem. Phys., 15, 6147-6158, 10.5194/acp-15-6147-2015, 2015.

Pratt, K. A., Twohy, C. H., Murphy, S. M., Moffet, R. C., Heymsfield, A. J., Gaston, C. J., DeMott, P. J.,
Field, P. R., Henn, T. R., Rogers, D. C., Gilles, M. K., Seinfeld, J. H., and Prather, K. A.: Observation of
playa salts as nuclei in orographic wave clouds, J. Geophys. Res.-Atmos., 115, D15301,
10.1029/2009jd013606, 2010.

Qi, J., Zheng, B., Li, M., Yu, F., Chen, C., Liu, F., Zhou, X., Yuan, J., Zhang, Q., and He, K.: A high-resolution air pollutants emission inventory in 2013 for the Beijing-Tianjin-Hebei region, China, Atmos. Environ., 170, 156-168, 10.1016/j.atmosenv.2017.09.039, 2017.

Qian, Y., Gong, D., Fan, J., Leung, L. R., Bennartz, R., Chen, D., and Wang, W.: Heavy pollution suppresses light rain in China: Observations and modeling, J. Geophys. Res.-Atmos., 114, D00K02, 10.1029/2008JD011575, 2009.

Riemer, N., and West, M.: Quantifying aerosol mixing state with entropy and diversity measures, Atmos. Chem. Phys., 13, 11423-11439, 10.5194/acp-13-11423-2013, 2013.

Roberts, J. R., Taylor, M. D., Castranova, V., Clarke, R. W., and Antonini, J. M.: Soluble metals associated with residual oil fly ash increase morbidity and lung injury after bacterial infection in rats, J. Toxicol. Env. Health Part A, 67, 251-263, 10.1080/15287390490266927, 2004.

Rosenfeld, D.: Suppression of rain and snow by urban and industrial air pollution, Science, 287, 1793-1796, 10.1126/science.287.5459.1793, 2000.

Rosenfeld, D., Sherwood, S., Wood, R., and Donner, L.: Climate effects of aerosol-cloud interactions, Science, 343, 379-380, 10.1126/science.1247490, 2014.

Roth, A., Schneider, J., Klimach, T., Mertes, S., van Pinxteren, D., Herrmann, H., and Borrmann, S.: Aerosol properties, source identification, and cloud processing in orographic clouds measured by single particle mass spectrometry on a central European mountain site during HCCT-2010, Atmos. Chem. Phys., 16, 505-524, 10.5194/acp-16-505-2016, 2016.

Schneider, J., Mertes, S., Pinxteren, D. v., Herrmann, H., and Borrmann, S.: Uptake of nitric acid, ammonia, and organics in orographic clouds: mass spectrometric analyses of droplet residual and interstitial aerosol particles, Atmos. Chem. Phys., 17, 1571-1593, 10.5194/acp-17-1571-2017, 2017.

Schroder, J., Hanna, S., Modini, R., Corrigan, A., Kreidenweis, S., Macdonald, A., Noone, K. J., Russell, L., Leaitch, W., and Bertram, A.: Size-resolved observations of refractory black carbon particles in cloud droplets at a marine boundary layer site, Atmos. Chem. Phys., 15, 1367-1383, 10.5194/acp-15-1367-2015, 2015.

Seinfeld, J. H., and Pandis, S. N.: Atmospheric chemistry and physics: from air pollution to climate change, John Wiley & Sons, 2006.

Seinfeld, J. H., Bretherton, C., Carslaw, K. S., Coe, H., DeMott, P. J., Dunlea, E. J., Feingold, G., Ghan, S., Guenther, A. B., Kahn, R., Kraucunas, I., Kreidenweis, S. M., Molina, M. J., Nenes, A., Penner, J. E.,

549 Prather, K. A., Ramanathan, V., Ramaswamy, V., Rasch, P. J., Ravishankara, A. R., Rosenfeld, D.,

550 Stephens, G., and Wood, R.: Improving our fundamental understanding of the role of aerosol-cloud

551 interactions in the climate system, Proc. Natl. Acad. Sci. U.S.A., 113, 5781-5790,

552 10.1073/pnas.1514043113, 2016.

553 Shen, X. H., Lee, T., Guo, J., Wang, X., Li, P., Xu, P., Wang, Y., Ren, Y., Wang, W., Wang, T., Li, Y.,

554 Cam, S. A., and Collett, J. L., Jr.: Aqueous phase sulfate production in clouds in eastern China, Atmos.

555 Environ., 62, 502-511, 10.1016/j.atmosenv.2012.07.079, 2012.

556 Tilgner, A., Schöne, L., Bräuer, P., Van Pinxteren, D., Hoffmann, E., Spindler, G., Styler, S., Mertes, S.,

557 Birmili, W., and Otto, R.: Comprehensive assessment of meteorological conditions and airflow

558 connectivity during HCCT-2010, Atmos. Chem. Phys., 14, 9105-9128, 10.5194/acp-14-9105-2014,

559 2014.

560 Twohy, C. H., and Anderson, J. R.: Droplet nuclei in non-precipitating clouds: composition and size

561 matter, Environ. Res. Lett., 3, 10.1088/1748-9326/3/4/045002, 2008.

562 Ueda, S., Hirose, Y., Miura, K., and Okochi, H.: Individual aerosol particles in and below clouds along a

563 Mt. Fuji slope: Modification of sea-salt-containing particles by in-cloud processing, Atmos. Res., 137,

564 216-227, 10.1016/j.atmosres.2013.10.011, 2014.

565 Wang, J., Cubison, M. J., Aiken, A. C., Jimenez, J. L., and Collins, D. R.: The importance of aerosol

566 mixing state and size-resolved composition on CCN concentration and the variation of the importance

567 with atmospheric aging of aerosols, Atmos. Chem. Phys., 10, 7267-7283, 10.5194/acp-10-7267-2010,

568 2010.

569 Wang, Y., Guo, J., Wang, T., Ding, A., Gao, J., Zhou, Y., Collett, J. L., and Wang, W.: Influence of

570 regional pollution and sandstorms on the chemical composition of cloud/fog at the summit of Mt.

571 Taishan in northern China, Atmos. Res., 99, 434-442, 10.1016/j.atmosres.2010.11.010, 2011.

572 Wang, Z., Zhang, H., Li, J., Jing, X., and Lu, P.: Radiative forcing and climate response due to the

573 presence of black carbon in cloud droplets, J. Geophys. Res.-Atmos., 118, 3662-3675,

574 10.1002/jgrd.50312, 2013.

575 Zhang, D., Ishizaka, Y., and Aryal, D.: Individual particles and droplets in continentally influenced

576 stratocumulus: A case study over the Sea of Japan, Atmos. Res., 79, 30-51,

577 10.1016/j.atmosres.2005.04.003, 2006.

578 Zhang, G., Lin, Q., Peng, L., Bi, X., Chen, D., Li, M., Li, L., Brechtel, F. J., Chen, J., Yan, W., Wang, X.,

579 Peng, P., amp, apos, an, Sheng, G., and Zhou, Z.: The single-particle mixing state and cloud scavenging

580 of black carbon: a case study at a high-altitude mountain site in southern China, Atmos. Chem. Phys.,

581 17, 14975-14985, 10.5194/acp-17-14975-2017, 2017.

582 Zhang, Y. M., Zhang, X. Y., Sun, J. Y., Hu, G. Y., Shen, X. J., Wang, Y. Q., Wang, T. T., Wang, D. Z.,

583 and Zhao, Y.: Chemical composition and mass size distribution of PM_1 at an elevated site in central east

584 China, Atmos. Chem. Phys., 14, 12237-12249, 10.5194/acp-14-12237-2014, 2014.

585 Zhao, C., Tie, X., and Lin, Y.: A possible positive feedback of reduction of precipitation and increase in

586 aerosols over eastern central China, Geophys. Res. Lett., 33, L11814, 10.1029/2006gl025959, 2006.

587 Zuberi, B., Johnson, K. S., Aleks, G. K., Molina, L. T., and Laskin, A.: Hydrophilic properties of aged

588 soot, Geophys. Res. Lett., 32, L01807, 10.1029/2004gl021496, 2005.

589